JAST (Journal of Animal Science and Technology) TITLE PAGE

Upload this completed form to website with submission

ARTICLE INFORMATION	Fill in information in each box below
Article Type	Research article
Article Title (within 20 words without abbreviations)	Transcriptomic Profiling of Porcine Duodenal, Jejunal, and Ileal Organoids in Response to Porcine Epidemic Diarrhea Virus
Running Title (within 10 words)	Transcriptomic Profiling of Porcine Intestinal Organoids in Response to PEDV
Author	Jiyoung Heo1†, Jae Han Park1†, Hyun Sung Park1, Dong-Hoon Chae1, Aaron Yu1, Keonwoo Cho1, Dong Ha Bhang2, Yoo Yong Kim1, Mi-Kyung Oh 1*, Kyung-Rok Yu1*
Affiliation	1 Department of Agricultural Biotechnology and Research Institute of Agriculture and Life Sciences, Seoul National University, Seoul 08826, Korea, Republic of 2 Attislab Inc., Anyang, Gyeonggi-Do 14059, Korea, Republic of
ORCID (for more information, please visit https://orcid.org)	Jiyoung Heo (https://orcid.org/0009-0001-7271-6708) Jae Han Park (https://orcid.org/0009-0003-8995-1944) Hyun Sung Park (https://orcid.org/0009-0008-8210-2823) Dong-Hoon Chae (https://orcid.org/0009-0007-7002-2992) Aaron Yu (https://orcid.org/0009-0003-0731-7422) Keonwoo Cho (https://orcid.org/0009-0006-2235-942X) Dong Ha Bhang (https://orcid.org/0000-0002-6727-4036) Yoo Yong Kim (https://orcid.org/0000-0001-8121-3291) Mi-Kyung Oh (https://orcid.org/0009-0009-7678-0027) Kyung-Rok Yu (https://orcid.org/0000-0002-4685-3223)
Competing interests	No potential conflict of interest relevant to this article was reported.
Funding sources State funding sources (grants, funding sources, equipment, and supplies). Include name and number of grant if available.	This work was supported by the National Research Foundation of Korea (NRF) funded by the Korea government (No. 2022R1C1C1009606), and the Basic Science Research Program through the National Research Foundation of Korea (NRF) funded by the Ministry of Education (No. 2022R1I1A1A01071265).
Acknowledgements	We appreciate Prof. Daesub Song (Seoul National University, Seoul, Korea) for their generous providing PEDV DR13 strain.
Availability of data and material	Upon reasonable request, the datasets of this study can be available from the corresponding author.
Authors' contributions Please specify the authors' role using this form.	Conceptualization: Oh MK, Yu KR. Data curation: Heo J, Park JH. Formal analysis: Heo J, Park JH. Methodology: Heo J, Park HS, Chae DH, Yu AR, Cho K, Bhang DH, Kim YY. Software: Park JH, Park HS. Validation: Heo J, Park JH, Oh MK, Yu KR. Investigation: Heo J, Park JH. Writing - original draft: Heo J, Park JH, Oh MK, Yu KR. Writing - review & editing: Heo J, Park JH, Park HS, Chae DH, Yu A, Cho K, Bhang DH, Kim YY, Oh MK, Yu KR.
Ethics approval and consent to participate	All procedures involving porcine were approved by the Seoul National University Institutional Animal Care and Use Committee (SNU-230915-4-1) and conducted in accordance with guidelines for the care and use of laboratory animals.

CORRESPONDING AUTHOR CONTACT INFORMATION

For the corresponding author (responsible for correspondence, proofreading, and reprints)	Fill in information in each box below
First name, middle initial, last name	Mi-Kyung Oh, Kyung-Rok Yu
Email address – this is where your proofs will be sent	ipomk@snu.ac.kr, cellyu@snu.ac.kr

Secondary Email address	
Address	Department of Agricultural Biotechnology and Research Institute of Agriculture and Life Sciences, Seoul National University, Seoul 08826, Korea
Cell phone number	+82-10-8477-6745, +82-10-3191-3171
Office phone number	+82-2-880-4816, +82-2-880-4807
Fax number	+82-2-873-2271

Abstract

Porcine epidemic diarrhea virus (PEDV) is a highly pathogenic virus that causes severe gastrointestinal disease in neonatal piglets, often leading to high mortality. To better understand PEDV pathogenesis, we developed porcine intestinal apical-out organoids derived from the duodenum, jejunum, and ileum that support viral replication and enable long-term experimental manipulation. In this study, we investigated the region-specific responses of these organoids to PEDV infection, focusing on regional characteristics, gene expression, and susceptibility to infection. PEDV replicated efficiently in the apical-out organoids, with significantly higher viral loads in jejunal and ileal organoids than duodenal organoids, indicating region-specific susceptibility. Bulk RNA sequencing and a differential gene expression analysis revealed unique transcriptomic responses across regions. The jejunal and ileal organoids exhibited stronger activation of pathways related to cellular processes, immune regulation, and antiviral defense than the duodenal organoids. Notably, viral entry receptor genes such as *ANPEP*, *ACE2*, and *DPP4* were expressed at higher levels in jejunal and ileal organoids under uninfected conditions, suggesting an innate predisposition for viral entry in these regions. Further analysis identified key upregulated genes involved in immune modulation, inflammation regulation, and tissue integrity, such as *SLIT2*, *MMD2*, and *PKHD1*, along with downregulated genes, including *IL-1A*, *MMP13*, and *GNA15*, that help control inflammation and minimize tissue damage. In conclusion, PEDV infection in porcine intestinal organoids elicits region-specific responses, with increased susceptibility and antiviral activation in jejunal and ileal organoids driven by the differential expression of viral entry receptors and immune-regulatory genes.

Keywords: Porcine epidemic diarrhea virus (PEDV), Porcine intestinal organoids, Gene expression profiling Region-specific responses, Viral pathogenesis

Introduction

Porcine epidemic diarrhea virus (PEDV) is a highly virulent pathogen that poses a significant threat to the swine industry, particularly to neonatal piglets [1-3]. PEDV infection causes severe gastrointestinal symptoms, including diarrhea, vomiting, and dehydration, which can lead to mortality rates approaching 100% in affected populations [4, 5]. The virus primarily targets the intestinal epithelium [6], particularly in the jejunum and ileum, leading to villous atrophy and compromised gut integrity [7]. Understanding PEDV pathogenesis is essential for developing effective therapeutic strategies and vaccines.

Traditionally, PEDV research has relied on two-dimensional (2D) cell-culture models, such as the IPEC-J2 and IPI-2I cell lines derived from porcine intestinal tissue [8, 9]. However, those models are limited in their ability to replicate the complex *in vivo* environment of the porcine intestine, which features diverse cell types, unique structural architecture, and region-specific physiological characteristics [10]. Recently, organoid technology has presented a promising alternative, allowing for the cultivation of three-dimensional (3D) organoids that more accurately mimic the physiological conditions of the intestinal epithelium [4, 11, 12]. Importantly, organoids can be derived from specific regions of the intestine, such as the duodenum, jejunum, and ileum, enabling the study of region-specific responses to PEDV infection [13].

Studies have shown that PEDV infection efficiency and host responses vary across intestinal segments, likely due to inherent differences among the duodenum, jejunum, and ileum [14, 15]. Furthermore, distinct gene expression patterns in the small intestine suggest that each region has specialized physiological functions that might influence its susceptibility to infection [16]. Despite the increasing use of organoids to study enteric viruses, few studies have investigated the region-specific gene expression responses to PEDV infection, and the influence of those differences on viral pathogenesis remains underexplored [17-19].

For this study, we established apical-out porcine intestinal organoids derived from the duodenum, jejunum, and ileum to investigate region-specific transcriptional and functional responses to PEDV infection. Specifically, we investigated how different intestinal regions responded to PEDV at the molecular level, identifying variations in gene expression profiles, immune activation, and antiviral defense mechanisms.

Materials and Methods

Animal and viruses

All procedures involving pigs were approved by the Seoul National University Institutional Animal Care and Use Committee (SNU-230915-4-1) and conducted in accordance with guidelines for the care and use of laboratory animals. The PEDV DR13 strain used in this study was generously provided by Professor Daesub Song from Seoul National University [20].

Cell culture

Vero cells were cultured in Dulbecco modified Eagle medium (DMEM, Biowest, Nuaillé, France) supplemented with 5% fetal bovine serum (FBS, Biowest) and 1% antibiotic-antimycotic (Gibco, Grand Island, NY, USA) in a 37 ℃ incubator supplied with 5% CO_2. Vero cells were subcultured at 70–80% confluency, and PEDV was inoculated when the cells reached 70–80% confluency.

Virus titration ($TCID_{50}$ assay)

The virus was propagated in Vero cells that were seeded one day before infection in a T-75 flask at 70–80% confluency and incubated overnight at 37 ℃ with 5% CO_2. The cells were washed once with phosphate-buffered saline (PBS, Biosesang, Korea) and inoculated with diluted PEDV DR13 for 1 h. Then the cells were washed once with PBS and maintained in the PEDV infection medium, which contained DMEM (Biowest) with 0.3% tryptose phosphate broth (BD Difco, Franklin Lakes, NJ, USA), 0.02% yeast extract (Gibco), 2 μg/mL TPCK trypsin (Thermo Scientific, Waltham, MA, USA), and 1% antibiotic-antimycotic (Gibco) at 37 ℃ in 5% CO_2. The cytopathic effects (CPE) were monitored daily, and the virus was harvested using three rounds of freezing and thawing after 72–96 h, when the CPE exceeded 80%. The cell supernatant was centrifuged at 4,000 rpm for 20 min, and then the supernatant of the sample was aliquoted and stored at -80 ℃ until use. The virus titer was measured using Vero cells that were seeded in 96-well plates at a density of 2×10^4 cells/well in 200 μL of culture medium and incubated at 37 ℃ in 5% CO_2. The virus was diluted in a 10-fold series in DMEM with 1% antibiotic-antimycotic. Each dilution was added to the well in six replicates, and the negative control cells were treated only with DMEM and 1% antibiotic-antimycotic. After 1 h of incubation with the virus, the cells were washed once with PBS and then maintained in the PEDV infection medium, as in the propagation procedure. After 72–96 h, when the CPE exceeded 80%, the mean tissue culture infection dose 50 ($TCID_{50}$) was calculated using the Spearman-Kärber method.

Porcine intestinal organoid culture and differentiation

Duodenum, jejunum, and ileum tissue from of small intestines of 1-week-old piglets was dissected, and crypts were isolated with Gentle cell dissociation reagent (StemCell Technologies, Vancouver, BC, Canada). Then, the crypts were embedded in Matrigel (Corning, NY, USA) with growth medium. The organoids were passaged every 4–5 days. To differentiate the porcine intestinal organoids, the culture medium was changed to differentiation medium after 2–3 days of passaging.

The porcine intestinal organoid growth medium was Advanced DMEM (Gibco) supplemented with 2 mM GlutaMAX, 10 mM HEPES (Gibco), 1% penicillin/streptomycin, 1X N-2 supplement, 1X B-27 supplement without vitamin A (Thermo Fisher), 500 ng/mL human R-spondin 1, 100 ng/mL human Noggin, 50 ng/mL human EGF (Peprotech, Rocky Hill, NJ, USA), 100 ng/mL WNT surrogate-Fc fusion protein (IPA, Victoria, BC, Canada), 0.5 µM A83-01, 10 µM SB202190, 10 mM nicotinamide, 10 nM human gastrin I, 5 µM LY2157299, 2.5 µM CHIR99021 (Sigma-Aldrich, St. Louis, MO, USA), and 10 µM Y-27632 (MedChem Express, Princeton, NJ, USA).

The porcine intestinal organoid differentiation medium contained reduced concentrations of human R-spondin 1, human Noggin, and WNT surrogate-Fc fusion protein (1/10 in the culture medium) and 10 mM DAPT (Sigma-Aldrich).

Apical-out porcine intestinal organoid culture

The organoids were passaged 2-3 days prior to starting the apical-out culture and were maintained in growth medium. Matrigel-embedded organoids have basolateral surfaces facing outward, which are referred to as basal-out organoids. To generate apical-out organoids, the organoids were first separated from the Matrigel by incubating them in 5 mM EDTA in PBS on a shaking rotor for 30 min at 4 ℃ to remove the extracellular matrix proteins. The organoids were centrifuged at 200 g for 5 min at 4 ℃. Then, the pellet was re-suspended in differentiation medium in ultra-low attachment 24-well cell culture plates (Corning). After transitioning to apical-out culture for 3 days, the suspended organoids exhibit reversed polarity, with the apical surfaces face outward. These are referred to as apical-out organoids.

Viral infection

We infected 200 apical-out organoids with PEDV DR13 for 1 h at 37 ℃. After 1 h, the medium containing the virus was removed, and differentiation medium was added.

The basal-out organoids were separated from the Matrigel and infected with PEDV DR13 in ultra-low attachment 24-well plates for 1 h at 37 ℃. After 1 h, these organoids were re-embedded in Matrigel, and differentiation medium was added. Sampling was conducted 24 h after inoculation.

RNA extraction and qRT-PCR analysis

The cultured apical-out organoids were harvested, and total RNA was extracted using Trizol reagent (Invitrogen, Carlsbad, USA). From each sample, 2 μg of RNA was taken and converted into cDNA using M-MLV reverse transcriptase (Promega, Madison, WI, USA). Real-time quantitative PCR was conducted as previously described [21] on a CFX Duet (Biorad, Hercules, CA, USA) with SYBR green master mix (Applied Biosystems, Foster City, CA, USA). Porcine *GAPDH* was used to normalize gene expression. The sequences of the primers used in this study are listed in Table 1.

Organoid immunofluorescence analysis

Organoids separated from the Matrigel were fixed in 4% paraformaldehyde for 20 min. For cryo-sectioning, the fixed organoids were embedded first in 30% sucrose and subsequently in a gelatin/sucrose solution. Immunocytochemistry staining was conducted on 12-μm sections of the gelatin-embedded organoids. These sections were incubated in blocking/permeabilization buffer (1.5 mL of FBS, 0.5 g of bovine serum albumin (BSA, LPS solution, Korea) 250 μL of Triton X-100, 250 μL of Tween 20, and 500 μL of 1% (wt/vol) sodium deoxycholate solution in 47.5 mL of PBS [22]) for 1 h at room temperature. Primary antibodies were then applied overnight at 4 ℃. After the samples were washed, secondary antibodies were applied for 2 h at room temperature. Then, the samples were counterstained with DAPI (Sigma-Aldrich) and mounted with fluorescence mounting medium (DAKO, Glostrup, Denmark). Fluorescent images were obtained using a Leica TCS SP8 X (Leica Microsystems, Wetzlar, Germany). The antibodies used in this study are listed in Table 2.

RNA-seq and analysis

Sequencing of the extracted RNA was performed at Macrogen Incorporated using the manufacturer's reagents and protocol. mRNA sequencing libraries were prepared from the extracted RNA by using an Illumina TruSeq stranded

mRNA sample prep kit (Illumina, Inc., San Diego, CA, USA). Indexed libraries of the samples were submitted to paired-end read sequencing on an Illumina NovaSeqX (Illumina, Inc.). The sequenced data were processed and analyzed with minor modifications to a previously described procedure [23]. Adapter sequences were removed and low-quality reads were filtered using Cutadapt (v4.9). The trimmed sequences were aligned to the *Sus scrofa* reference genome (susScr2) using HISAT2 (v2.2.1) and counted by featureCounts (v2.0.3). Gene expression was quantified by EdgeR (v3.36.0), and differentially expressed genes (DEGs) were further analyzed. We identified DEGs using absolute log2 fold change ≥ 1 and *p*-values<0.05 as the threshold. For the Gene Ontology (GO) analysis of DEGs, PANTHER19.0 [24] was used to categorize the genes into Panther GO terms. The DEGs were also annotated into KEGG database pathways using ShinyGO 0.81 (http://bioinformatics.sdstate.edu/go/) [25, 26]. Volcano plots of the DEGs were generated with ggplot 2 in R. A principal component analysis (PCA) plot and heatmaps were generated using an in-house script in R. For the heatmaps, the samples were clustered according to Euclidean distance. Proportional Venn diagrams of up- and downregulated genes were created using BioVenn [27]. The RNA-seq data presented in this study have been deposited in the NCBI GEO database under accession number GSE 280630.

Statistical analysis

All experiments were performed in at least triplicate. Depending on the number of groups to be compared, t-tests and one-way ANOVA were used to analyze the data. The values are represented as the mean ± SEM. A *p*-value of less than 0.05 were considered statistically significant. All statistical analyses were performed using GraphPad Prism software (v8.0.1).

Table 1. List of primers used in this study

Porcine		
Gene	Forward	Reverse
GAPDH	CTGCCCAGAACATCATCCC	CAGTGAGCTTCCCGTTGAG
CYBRD1	ACAGCTTCAAGAAGTCGACGC	GCCAGGAAACCCCTGTAACC
SLC40A1	GCCTTAACCGTTCATGCACTT	GTGGGGAATGCAATTCAGGA
LCT	GCTGATCATGCTTGAAATTTTGC	CTGCACAAGTTTCTGACGGT
SLC10A2	CCAGAGTGCCTGGATCATCG	GTTTCCAGAGCAACCGTTCG
OSTB	AGTCCTTTGTCCTATGCTGGC	CAGAACCTTCGCTGTCCCT
MUC2	GGACGCCTACAAGGAGTTCG	ACCAGCTGCTGAGTGAGGTA
LYZ	CCCGGCTTCTCAGACAACAT	CCTATAGCCGTCCATGCCAG
VIL1	CCTCCCCTAGACAGGCTCATC	ACCATCTGCATGGCCTCTATC
CHGA	GTCATTGCCCTCCCTGTGAA	TCAAAACACTCCTGGCTGACA
PEDV M	GGTTCTATTCCCGTTGATGAGGT	AACACAAGAGGCCAAAGTATCCAT
CXCL9	TAAACAATTCGCCCCAAGCC	CATGGTCCCTCATGTCATCTTC
CXCL10	CCCACATGTTGAGATCATTGC	CATCCTTATCAGTAGTGCCG
IL17	CTCGTGAAGGCGGGAATCAT	GGTGTGCTCCGGTTCAAGAT
ISG15	CTATGAGGTCTGGCTGACGC	ACGGTGCACATAGGCTTGAG
ISG58	ATTTGCCTACACGGACCTGG	GCGACCATAGTGGTAGTGGA
IFNL3	GGATGCCTTTGAAGAGTCCCT	GCTGTGCAGGGATGAGTTCG

164 **Table 2. Antibodies**

Protein	Company	Application	Dilution
ZO-1	Santa Cruz (sc-33725)	ICC	1:100
Villin	Santa Cruz (sc-58897)	ICC	1:100
Chromogranin A	Abcam (ab15160)	ICC	1:100
Ki67	DAKO (M7240)	ICC	1:100
PEDV N	AntibodySystem (PVV28802)	ICC	1:100
Anti-mouse IgG (H+L), F(ab') 2 Fragment (Alexa Fluor (R) 488 Conjugate)	Cell Signaling (4408S)	ICC	1:500
Anti-rabbit IgG(H+L), F(ab') 2 Fragment (Alexa Fluor (R) 488 Conjugate)	Cell Signaling (4412S)	ICC	1:500
Anti-mouse IgG (H+L), F(ab') 2 Fragment (Alexa Fluor (R) 594 Conjugate)	Cell Signaling (8890S)	ICC	1:500
Goat Anti-rat IgG H&L (Alexa Fluor 594)	Abcam (ab150160)	ICC	1:500
DAPI	Sigma-Aldrich (D9542)	ICC	1:1000

165

Results

Establishment and characterization of porcine duodenal, jejunal, and ileal organoids

To develop an *in vitro* model of the porcine intestine, we established organoids derived from the duodenum, jejunum, and ileum. A microscopy morphological analysis revealed distinct structural features in the organoids from each region, with duodenal organoids resembling the structure of gastric organoids and showing morphological differences from the jejunal and ileal organoids (Fig. 1A). The proliferation analysis showed significantly lower proliferation rates in the duodenal organoids than in the jejunal and ileal organoids (Fig. 1B). Consistent with previous findings, these structural and functional differences across regions could contribute to differential responses to PEDV infection [14, 15]. The qRT-PCR analysis of region-specific markers confirmed the establishment of region-specific organoids: the duodenal organoids expressed high levels of *CYBRD1* and *SLC40A1*, jejunal organoids showed elevated levels of *LCT*, and ileal organoids had increased expression of *SLC10A2* and *OSTB* (Fig. 1C). Immunofluorescence staining revealed consistent expression of the enterocyte marker Villin and the enteroendocrine marker CHGA (chromogranin A) across all three region-derived organoids (Fig. 1D). Notably, enterocytes, the primary target of PEDV, were present in all organoids, indicating that the developed organoids closely replicate the *in vivo* porcine intestine environment.

Porcine intestinal organoids show regional differences in PEDV replication and host response

To investigate PEDV replication and host responses, we cultured apical-out and basal-out organoids derived from the duodenum, jejunum, and ileum. Immunofluorescence staining was performed to assess polarity, and it showed the apical marker ZO-1 on the outer membrane in the apical-out organoids and the inner membrane in the basal-out organoids, confirming the correct polarity. Additionally, the proliferation marker Ki67 was more prominent in the jejunal and ileal organoids, aligning with the proliferation patterns observed in Fig. 1B (Fig. 2A). To characterize the cell composition, we analyzed the expression of cell-specific markers by qRT-PCR and found no significant differences between the basal-out and apical-out organoids. Goblet cell (*MUC2*), Paneth cell (*LYZ*), enterocyte (*VIL1*), and enteroendocrine cell (*CHGA*) markers were all detected, indicating the presence of diverse cell types across organoids of both polarities in each intestinal region (Fig 2B). The PEDV genomic RNA analysis showed more robust PEDV replication in the apical-out organoids, particularly the jejunal and ileal organoids, than in the basal-out and duodenal organoids (Fig. 2C). To assess host responses to PEDV infection, the expression levels of inflammation-related markers (*CXCL9, CXCL10, IL17*) and interferon pathway genes (*ISG15*, *ISG58*, *IFNL3*) were

measured. These markers were less expressed in the duodenal organoids than in the jejunal and ileal organoids (Fig. S1A), suggesting that the jejunal and ileal organoids were more responsive to PEDV infection.

RNA sequencing reveals regional differences in transcriptomic responses to PEDV in porcine intestinal organoids

To further investigate regional responses to PEDV at the transcriptomic level, we performed RNA sequencing on apical-out organoids from each region (Fig. 3A). The PCA demonstrated distinct transcriptomic profiles by region and infection status, indicating unique regional responses to PEDV infection (Fig. 3B and S2A–S2C). Heatmap clustering indicated close gene expression profiles between jejunal and ileal organoids, with duodenal organoids forming a separate cluster, even in the absence of infection (Fig. 3C). Notably, key receptors and entry-related genes (*ANPEP*, *ACE2*, and *DPP4*) were more highly expressed in jejunal and ileal organoids than in duodenal organoids in mock conditions, as were the proteases *TMPRSS4* and *TMPRSS11F*, which facilitate viral entry (Fig.3D). These findings suggest region-specific baseline gene expression profiles and receptor availability that might influence PEDV susceptibility.

PEDV infection induces region-specific gene expression changes in porcine intestinal organoids

To investigate region-specific transcriptional responses to PEDV infection, we analyzed DEGs in the duodenal, jejunal, and ileal organoids. A total of 20,428 genes were profiled, and DEGs with significant changes between the PEDV-infected and mock groups were identified using a threshold of $p<0.05$ and $|\log2 \text{ fold change}| \geq 1$. A volcano plot shows significant upregulation and downregulation of genes across regions (Fig. 4A). Specifically, the duodenum exhibited 58 upregulated and 40 downregulated genes, the jejunum had 101 upregulated and 261 downregulated genes, and the ileum had 67 upregulated and 131 downregulated genes (Fig. 4B). The GO enrichment analysis revealed region-specific functional categories among the DEGs. The jejunal and ileal organoids showed enrichment in GO terms related to cellular processes, biological regulation, metabolic activity, and membrane components, and the duodenal organoids had fewer gene counts in those enriched terms (Fig. 4C).

The KEGG pathway analysis further highlighted these region-specific responses. In the duodenum, the upregulated genes were associated with metabolic pathways and the renin-angiotensin system, and the downregulated genes were linked to PPAR signaling (Fig. 4D). In the jejunum, the upregulated genes were enriched in cytokine–cytokine receptor interactions and PI3K-Akt signaling, and the downregulated genes were involved in metabolic pathways and protein digestion and absorption (Fig. 4E). In the ileum, the upregulated genes were associated with metabolic

pathways and the glucagon signaling pathway, and the downregulated genes were linked to the MAPK signaling pathway and cytokine–cytokine receptor interactions (Fig. 4F). These findings demonstrate distinct transcriptional responses to PEDV infection across intestinal regions, with each segment activating unique pathways.

Regional gene expression patterns reveal key immune and cellular responses to PEDV in the jejunal and ileal organoids

To further investigate the regional differences in gene expression responses to PEDV infection, we identified the top 20 genes upregulated and downregulated in the duodenal, jejunal, and ileal organoids, compared with the mock groups. A heatmap analysis revealed distinct expression patterns across regions (Fig. 5A). In PEDV-infected duodenal organoids, upregulated genes such as *SNORA30* (viral processes), *TRIM72* (viral restriction), *WNT3* (Wnt/β-catenin signaling), and *PDE4B* (inflammatory response) suggest an immune response, and downregulated genes such as *PFKFB3* (carbohydrate metabolism) and *MMP1* (extracellular matrix remodeling) indicate reduced metabolic and cellular activity. In the jejunal organoids, genes such as *IL12R* (immune response), *GSDMA* (cell death), and *SPHK1* (sphingolipid metabolism) were upregulated, reflecting active immune and inflammatory responses, and the downregulated genes, such as *NLRC3* (PI3K-mTOR inhibition) and *MERTK* (viral entry), point to modulated immune signaling. In the ileal organoids, upregulated genes such as *STEAP4* (antiviral response), *PABPC4L* (coronavirus inhibition), *PLCβ2* (inflammation regulation), and *CTSW* (viral escape mechanisms) indicate robust immune activation, and the downregulated genes, such as *NCF1* and *S100A8* (inflammation modulation), show an adjusted inflammatory response. Venn diagrams of the DEGs reveal regional specificity, with three genes (*SLIT2*, *MMD2*, and *PKHD1*) commonly upregulated in the jejunal and ileal organoids (Fig. 5B). *SLIT2* reduces inflammation and tissue damage, and *PKHD1* supports epithelial barrier integrity, reflecting a coordinated response to maintain immune balance and tissue resilience in these regions. Among the 8 genes most commonly downregulated in the jejunal and ileal organoids (Fig. 5C), *IL-1A*, *MMP13*, and *GNA15* are involved in immune regulation and viral response, indicating inflammation and an antiviral response to PEDV infection. These commonly altered genes likely play key roles in the jejunum and ileum, where PEDV infection is prominent.

Discussion

This study provides critical insights into the region-specific responses of porcine intestinal organoids derived from the duodenum, jejunum, and ileum to PEDV infection. Using an apical-out organoid model, we observed distinct

functional responses to PEDV across these intestinal regions, suggesting that the jejunum and ileum might be especially critical for PEDV pathogenesis in neonatal piglets. These findings indicate that regional susceptibility to PEDV is influenced not only by anatomical differences but also by the unique transcriptomic profiles of each segment.

Our quantitative analysis revealed significantly higher PEDV replication in jejunal and ileal organoids than in duodenal organoids, supporting our hypothesis that susceptibility is modulated by region-specific gene expression patterns. Bulk RNA sequencing confirmed a more robust activation of immune and antiviral pathways in the jejunum and ileum, implying an elevated capacity for viral response in these regions. This finding aligns with other studies that show differential immune responses across intestinal segments, which could inform more effective intervention strategies [14, 28, 29].

Recent studies indicate that aminopeptidase N (APN) alone does not fully account for PEDV entry because infection persists in APN-knockout cells and pigs [30-32]. Our findings corroborate that, showing that the jejunal and ileal organoids had significantly higher baseline expression of viral entry receptor genes, including *ANPEP*, *ACE2*, and *DPP4*, and suggesting that, beyond APN, other known coronavirus receptors such as DPP4 and ACE2 might contribute to heightened intestinal infection. These findings are consistent with previous studies showing that *DPP4* and *ANPEP* expression is elevated in the jejunum compared with other regions [16, 33]. Additionally, the increased expression of proteases such as *TMPRSS4* and *TMPRSS11F* in these segments likely contributes to their increased susceptibility to PEDV, highlighting the importance of receptor availability in determining viral tropism [34, 35].

In response to PEDV infection, we observed significant regulation of genes involved in immune modulation and tissue integrity. Notably, *SLIT2*, *MMD2*, and *PKHD1* were upregulated in the jejunal and ileal organoids, suggesting a coordinated response to control inflammation and maintain tissue structure. *SLIT2* has been recognized for its anti-inflammatory properties, suggesting that its upregulation could play a critical role in balancing immune activation with tissue preservation during PEDV infection [36]. The downregulation of pro-inflammatory genes such as *IL-1A* and *MMP13* further indicates a protective mechanism that limits tissue damage [37-40]. This expression pattern supports a finely tuned immune response that promotes effective antiviral activity while preserving tissue integrity, positioning the jejunal and ileal regions as crucial sites of balanced, protective immune responses during PEDV infection.

This study highlights the utility of 3D organoid models in representing region-specific PEDV infection dynamics more accurately than traditional 2D models. While our focus was on porcine intestinal organoids, comparing our

findings with human and other animal models offers broader insights. For example, receptors like ACE2 and DPP4 are not only involved in PEDV entry in pigs but also play a significant role in the entry of coronaviruses such as SARS-CoV-2 in humans. Similar upregulation patterns of these receptors have been observed in both species, indicating conserved mechanisms of viral entry. Understanding these cross-species similarities and differences may refine therapeutic strategies and broaden our comprehension of coronavirus-host interactions. Our findings suggest that therapeutic strategies might be optimized by tailoring them to target specific intestinal regions, particularly the jejunum and ileum, where PEDV susceptibility is high. However, our current organoid model lacks immune cells, which are essential for simulating in vivo immune responses. Interactions between the intestinal epithelium and immune cells such as T cells, macrophages, and dendritic cells are crucial for mediating host responses to viral infections [41, 42]. The absence of these components may limit the model's ability to fully replicate immune-mediated aspects of PEDV pathogenesis. Future studies could enhance these models by incorporating immune cells to better reflect *in vivo* conditions. Additionally, co-culturing with other tissue organoids may provide a more comprehensive system to investigate the systemic effects of PEDV across multiple tissues."

In conclusion, this study elucidates the region-specific responses of porcine intestinal organoids to PEDV infection, demonstrating increased susceptibility and antiviral activation in jejunal and ileal organoids. These region-specific responses, driven by differential expression of viral entry receptors and immune-regulatory genes, advance our understanding of PEDV pathogenesis and suggest potential therapeutic targets for protecting neonatal piglets from PEDV.

Acknowledgments

We appreciate Prof. Daesub Song (Seoul National University) for generously providing the PEDV DR13 strain.

References

1. Saif LJ, Wang Q, Vlasova AN, Jung K, Xiao S. Coronaviruses. Diseases of swine. 2019:488-523.

2. Jung K, Saif LJ, Wang Q. Porcine epidemic diarrhea virus (PEDV): An update on etiology, transmission, pathogenesis, and prevention and control. Virus Research. 2020;286:198045.

3. Song D, Park B. Porcine epidemic diarrhoea virus: a comprehensive review of molecular epidemiology, diagnosis, and vaccines. Virus Genes. 2012;44(2):167-75.

4. Zhang M, Lv L, Cai H, Li Y, Gao F, Yu L, et al. Long-Term Expansion of Porcine Intestinal Organoids Serves as an in vitro Model for Swine Enteric Coronavirus Infection. Front Microbiol. 2022;13:865336.

5. Shamsi TN, Yin J, James ME, James MN. Porcine epidemic diarrhea: causative agent, epidemiology, clinical characteristics, and treatment strategy targeting main protease. Protein and Peptide Letters. 2022;29(5):392-407.

6. Segrist E, Cherry S. Using diverse model systems to define intestinal epithelial defenses to enteric viral infections. Cell host & microbe. 2020;27(3):329-44.

7. Jung K, Saif LJ. Porcine epidemic diarrhea virus infection: Etiology, epidemiology, pathogenesis and immunoprophylaxis. Vet J. 2015;204(2):134-43.

8. Wang X, Fang L, Liu S, Ke W, Wang D, Peng G, et al. Susceptibility of porcine IPI-2I intestinal epithelial cells to infection with swine enteric coronaviruses. Veterinary microbiology. 2019;233:21-7.

9. Jung K, Miyazaki A, Hu H, Saif LJ. Susceptibility of porcine IPEC-J2 intestinal epithelial cells to infection with porcine deltacoronavirus (PDCoV) and serum cytokine responses of gnotobiotic pigs to acute infection with IPEC-J2 cell culture-passaged PDCoV. Veterinary microbiology. 2018;221:49-58.

10. Koonpaew S, Teeravechyan S, Frantz PN, Chailangkarn T, Jongkaewwattana A. PEDV and PDCoV Pathogenesis: The Interplay Between Host Innate Immune Responses and Porcine Enteric Coronaviruses. Frontiers in Veterinary Science. 2019;6.

11. Ma P, Fang P, Ren T, Fang L, Xiao S. Porcine Intestinal Organoids: Overview of the State of the Art. Viruses. 2022;14(5).

12. Liu Y, Tan J, Zhang N, Li W, Fu B. A Strainer-Based Platform for the Collection and Immunolabeling of Porcine Epidemic Diarrhea Virus-Infected Porcine Intestinal Organoid. International Journal of Molecular Sciences. 2023;24(21):15671.

13. Li L, Fu F, Guo S, Wang H, He X, Xue M, et al. Porcine Intestinal Enteroids: a New Model for Studying Enteric Coronavirus Porcine Epidemic Diarrhea Virus Infection and the Host Innate Response. Journal of Virology. 2019;93(5):10.1128/jvi.01682-18.

14. Li Y, Wu Q, Huang L, Yuan C, Wang J, Yang Q. An alternative pathway of enteric PEDV dissemination from nasal cavity to intestinal mucosa in swine. Nature Communications. 2018;9(1):3811.

15. Yin L, Chen J, Li L, Guo S, Xue M, Zhang J, et al. Aminopeptidase N Expression, Not Interferon Responses, Determines the Intestinal Segmental Tropism of Porcine Deltacoronavirus. Journal of Virology. 2020;94(14):10.1128/jvi.00480-20.

16. Mach N, Berri M, Esquerré D, Chevaleyre C, Lemonnier G, Billon Y, et al. Extensive Expression Differences along Porcine Small Intestine Evidenced by Transcriptome Sequencing. PLOS ONE. 2014;9(2):e88515.

17. Lee S-A, Lee HJ, Gu N-Y, Park Y-R, Kim E-J, Kang S-J, et al. Evaluation of porcine intestinal organoids as an in vitro model for mammalian orthoreovirus 3 infection. J Vet Sci. 2023;24(4).

18. Li Y, Yang N, Chen J, Huang X, Zhang N, Yang S, et al. Next-Generation Porcine Intestinal Organoids: an Apical-Out Organoid Model for Swine Enteric Virus Infection and Immune Response Investigations. Journal of Virology. 2020;94(21):10.1128/jvi.01006-20.

19. Yen L, Nelli RK, Twu N-C, Mora-Díaz JC, Castillo G, Sitthicharoenchai P, et al. Development and characterization of segment-specific enteroids from the pig small intestine in Matrigel and transwell inserts: insights into susceptibility to porcine epidemic diarrhea Virus. Frontiers in Immunology. 2024;15.

20. Song DS, Oh JS, Kang BK, Yang JS, Moon HJ, Yoo HS, et al. Oral efficacy of Vero cell attenuated porcine epidemic diarrhea virus DR13 strain. Research in Veterinary Science. 2007;82(1):134-40.

21. Joo H, Oh M-K, Kang JY, Park HS, Chae D-H, Kim J, et al. Extracellular Vesicles from Thapsigargin-Treated Mesenchymal Stem Cells Ameliorated Experimental Colitis via Enhanced Immunomodulatory Properties. Biomedicines. 2021;9(2):209.

22. Wimmer RA, Leopoldi A, Aichinger M, Kerjaschki D, Penninger JM. Generation of blood vessel organoids from human pluripotent stem cells. Nature Protocols. 2019;14(11):3082-100.

23. Park HS, Lee B-C, Chae D-H, Yu A, Park JH, Heo J, et al. Cigarette smoke impairs the hematopoietic supportive property of mesenchymal stem cells via the production of reactive oxygen species and NLRP3 activation. Stem Cell Research & Therapy. 2024;15(1):145.

24. Thomas PD, Ebert D, Muruganujan A, Mushayahama T, Albou L-P, Mi H. PANTHER: Making genome-scale phylogenetics accessible to all. Protein Science. 2022;31(1):8-22.

25. Ge SX, Jung D, Yao R. ShinyGO: a graphical gene-set enrichment tool for animals and plants. Bioinformatics. 2019;36(8):2628-9.

26. Kanehisa M, Furumichi M, Sato Y, Ishiguro-Watanabe M, Tanabe M. KEGG: integrating viruses and cellular organisms. Nucleic Acids Research. 2020;49(D1):D545-D51.

27. Hulsen T, de Vlieg J, Alkema W. BioVenn – a web application for the comparison and visualization of biological lists using area-proportional Venn diagrams. BMC Genomics. 2008;9(1):488.

28. Liang J, Li Y, Yan Z, Jiao Z, Peng D, Zhang W. Study of the effect of intestinal immunity in neonatal piglets coinfected with porcine deltacoronavirus and porcine epidemic diarrhea virus. Arch Virol. 2022;167(8):1649-57.

29. Sun Y, Gong T, Wu D, Feng Y, Gao Q, Xing J, et al. Isolation, identification, and pathogenicity of porcine epidemic diarrhea virus. Frontiers in Microbiology. 2023;14.

30. Cui T, Theuns S, Xie J, Van den Broeck W, Nauwynck HJ. Role of Porcine Aminopeptidase N and Sialic Acids in Porcine Coronavirus Infections in Primary Porcine Enterocytes. Viruses. 2020;12(4).

31. Luo L, Wang S, Zhu L, Fan B, Liu T, Wang L, et al. Aminopeptidase N-null neonatal piglets are protected from transmissible gastroenteritis virus but not porcine epidemic diarrhea virus. Scientific Reports. 2019;9(1):13186.

32. Zhang J, Wu Z, Yang H. Aminopeptidase N Knockout Pigs Are Not Resistant to Porcine Epidemic Diarrhea Virus Infection. Virologica Sinica. 2019;34(5):592-5.

33. Saleem W, Ren X, Van Den Broeck W, Nauwynck H. Changes in intestinal morphology, number of mucus-producing cells and expression of coronavirus receptors APN, DPP4, ACE2 and TMPRSS2 in pigs with aging. Vet Res. 2023;54(1):34.

34. Zang R, Castro MFG, McCune BT, Zeng Q, Rothlauf PW, Sonnek NM, et al. TMPRSS2 and TMPRSS4 promote SARS-CoV-2 infection of human small intestinal enterocytes. Science Immunology. 2020;5(47):eabc3582.

35. Callies LK, Tadeo D, Simper J, Bugge TH, Szabo R. Iterative, multiplexed CRISPR-mediated gene editing for functional analysis of complex protease gene clusters. Journal of Biological Chemistry. 2019;294(44):15987-96.

36. Zhao H, Anand AR, Ganju RK. Slit2–Robo4 pathway modulates lipopolysaccharide-induced endothelial inflammation and its expression is dysregulated during endotoxemia. The Journal of Immunology. 2014;192(1):385-93.

37. Saeng-Chuto K, Madapong A, Kaeoket K, Piñeyro PE, Tantituvanont A, Nilubol D. Co-infection of porcine deltacoronavirus and porcine epidemic diarrhea virus induces early TRAF6-mediated NF-κB and IRF7 signaling pathways through TLRs. Sci Rep. 2022;12(1):19443.

38. Koop K, Enderle K, Hillmann M, Ruspeckhofer L, Vieth M, Sturm G, et al. Interleukin 36 receptor-inducible matrix metalloproteinase 13 mediates intestinal fibrosis. Frontiers in Immunology. 2023;14.

39. Cavalli G, Colafrancesco S, Emmi G, Imazio M, Lopalco G, Maggio MC, et al. Interleukin 1α: a comprehensive review on the role of IL-1α in the pathogenesis and treatment of autoimmune and inflammatory diseases. Autoimmunity Reviews. 2021;20(3):102763.

40. McEntee CP, Finlay CM, Lavelle EC. Divergent Roles for the IL-1 Family in Gastrointestinal Homeostasis and Inflammation. Front Immunol. 2019;10:1266.

41. Krishna VD, Kim Y, Yang M, Vannucci F, Molitor T, Torremorell M, et al. Immune responses to porcine epidemic diarrhea virus (PEDV) in swine and protection against subsequent infection. PLoS One. 2020;15(4):e0231723.

42. Yu H, Chen G, Zhang T, Huang X, Lu Y, Li M, et al. PEDV promotes the differentiation of CD4+ T cells towards Th1, Tfh, and Treg cells via CD103+ DCs. Virology. 2023;587:109880.

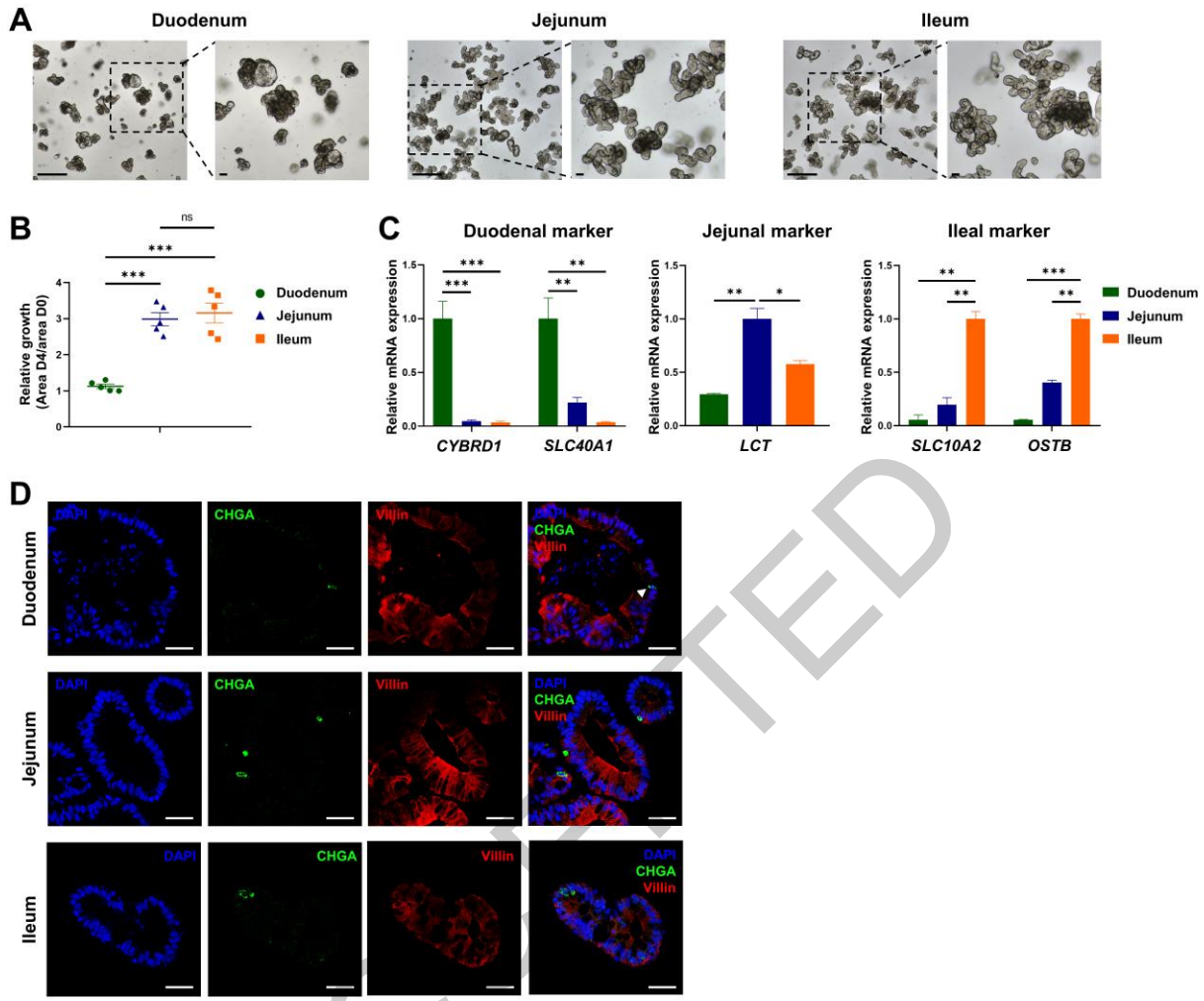

Figure 1. Establishment and characterization of mature porcine intestinal organoids

(A) Morphology of porcine duodenal, jejunal, and ileal organoids (Scale bar: 500 μm). (B) Quantification of organoid proliferation in the duodenal, jejunal, and ileal regions, measured by the ratio of the area on day 4 to that on day 0. (C) Gene expression of region-specific markers in duodenal (*CYBRD1* and *SLC40A1*), jejunal (*LCT*), and ileal (*SLC10A2* and *OSTB*) organoids was measured by qRT-PCR. The results are represented as the mean ± SEM (* $p<0.05$; ** $p<0.01$; *** $p<0.001$). (D) Protein expression of the enterocyte marker Villin and the enteroendocrine cell marker CHGA in duodenal, jejunal, and ileal organoids was detected with a confocal immunofluorescence analysis (Scale bar: 150 μm).

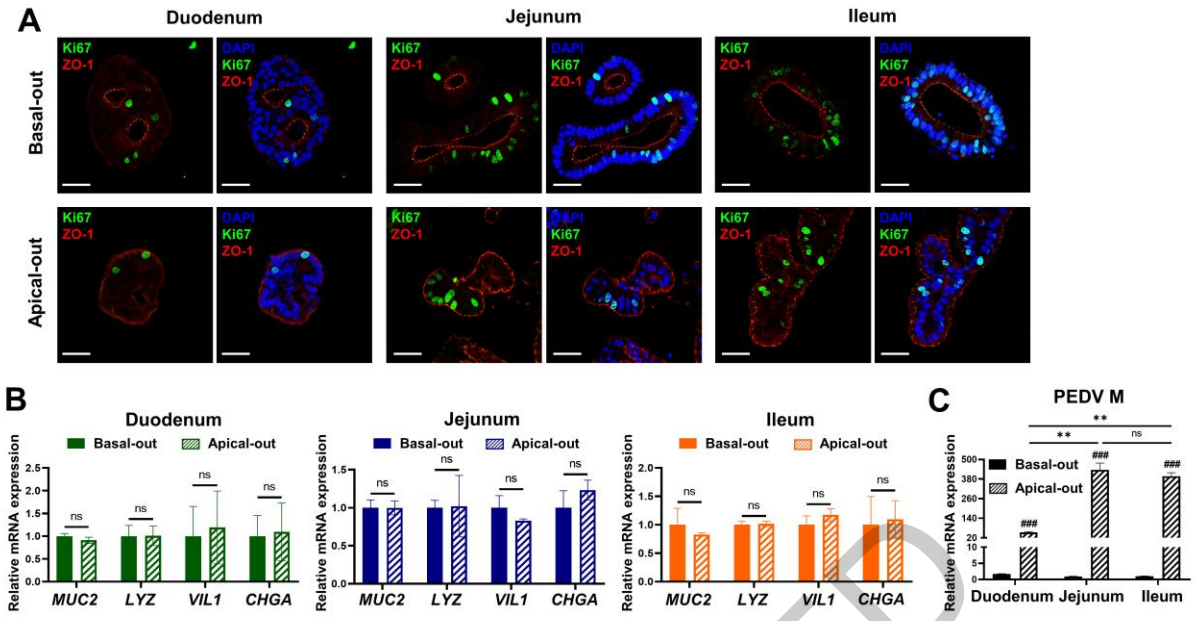

Figure 2. Replication of PEDV in apical-out porcine organoids

(A) Basal-out and apical-out duodenal, jejunal, and ileal organoids were stained for the apical protein marker ZO-1 and the proliferation marker Ki67 and visualized by confocal immunofluorescence (Scale bar: 150 μm). (B) Gene expression of the goblet cell marker (*MUC2*), Paneth cell marker (*LYZ*), enterocyte marker (*VIL1*), and enteroendocrine cell marker (*CHGA*) in basal-out and apical-out organoids was measured by qRT-PCR. (C) Genomic level of replicated PEDV in PEDV-infected basal-out and apical-out organoids was measured by qRT-PCR. The results are represented as the mean ± SEM (** p<0.01; ### p<0.001). (D) PEDV-infected apical-out porcine duodenal, jejunal, and ileal organoids were detected in a confocal immunofluorescence analysis (Scale bar: 150 μm).

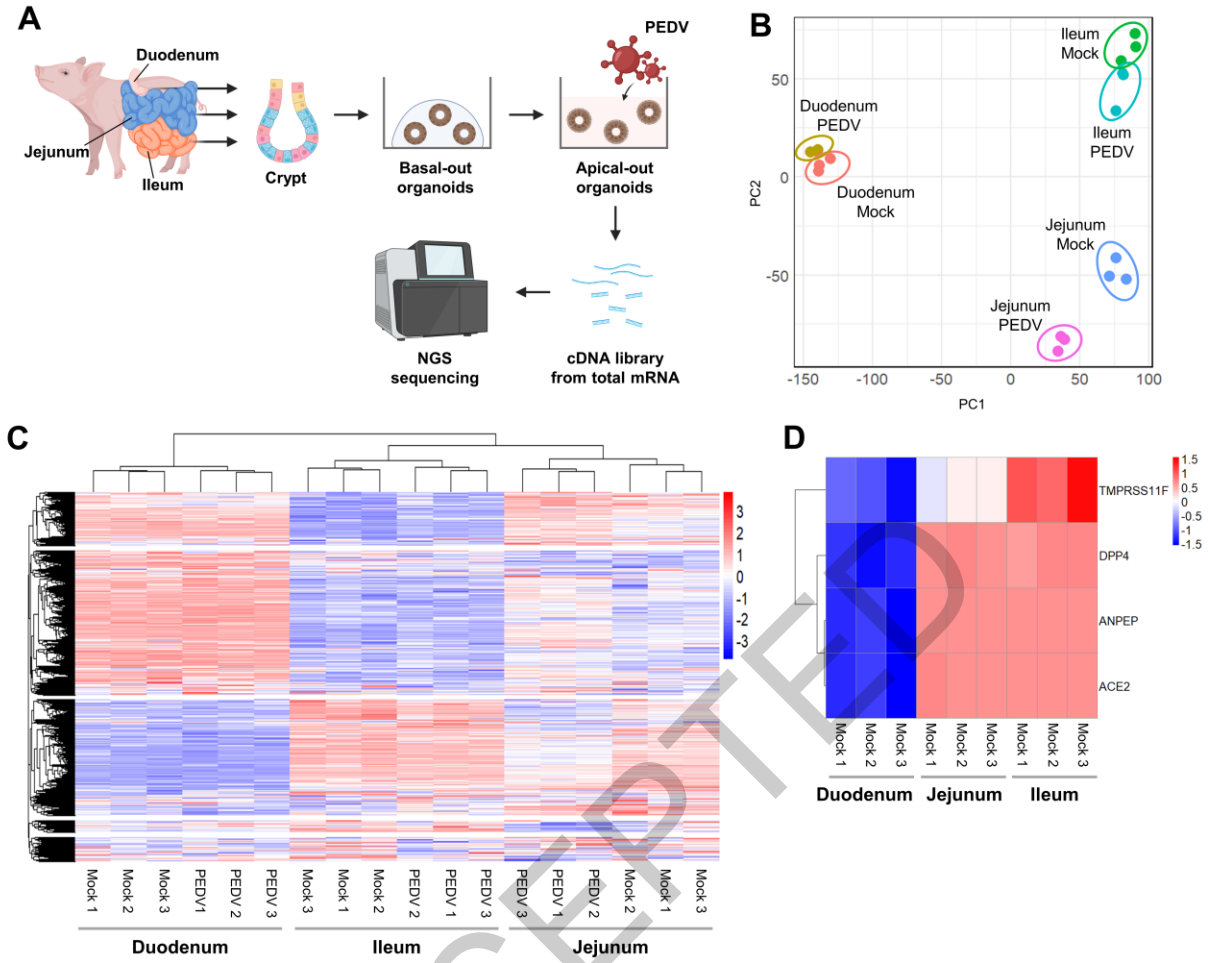

Figure 3. RNA sequencing analysis of duodenal, jejunal, and ileal organoids

(A) Diagrammatic representation of the experimental design. (B) Principal component analysis (PCA) of the gene expression profiles in duodenal, jejunal, and ileal organoids, based on bulk RNA sequencing data. (C) Heatmap of gene expression in duodenal, jejunal, and ileal organoids in the mock-infected and PEDV groups. (D) Heatmap showing the expression of coronavirus receptor and infection-related genes in mock-infected duodenal, jejunal, and ileal organoids.

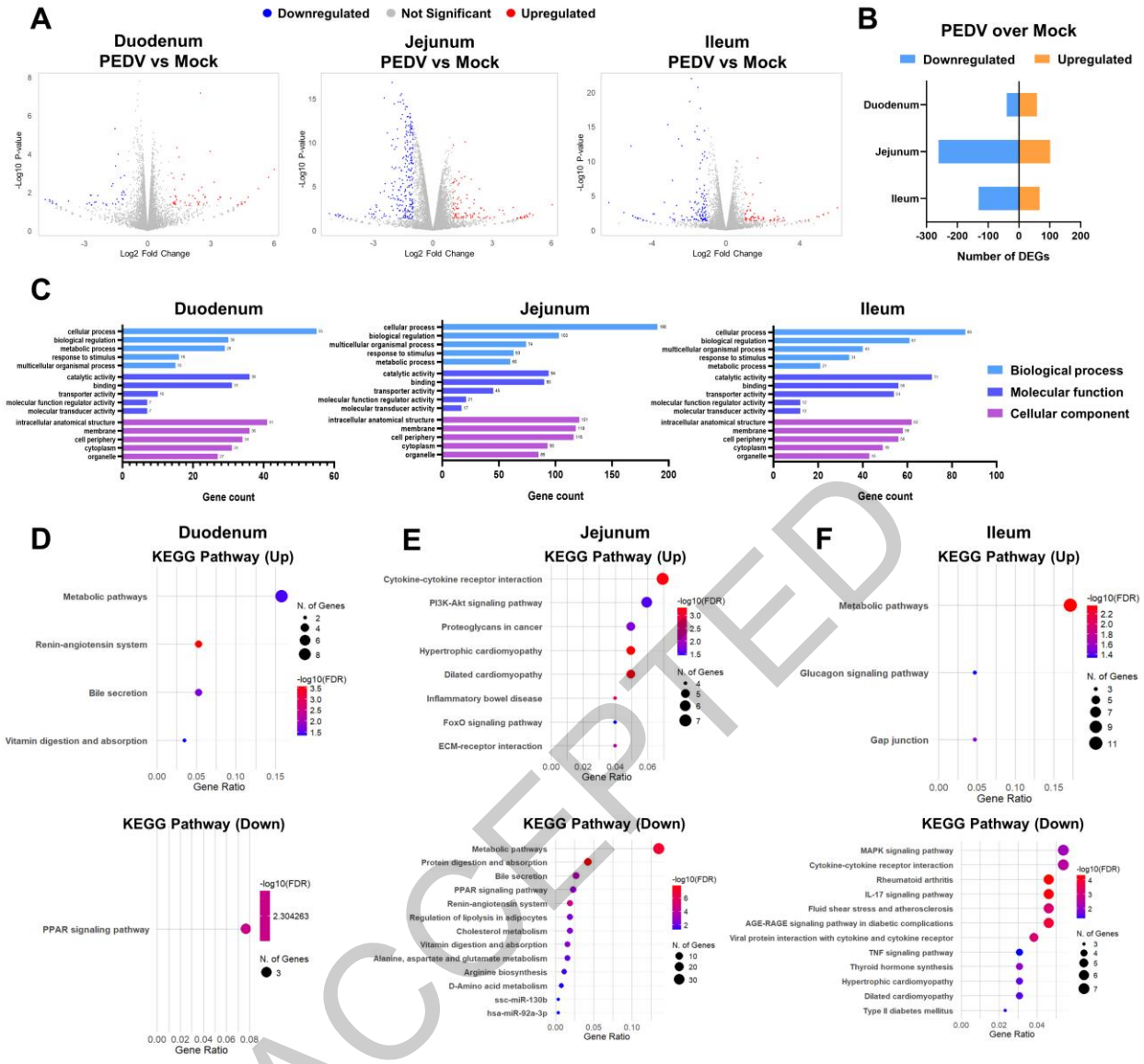

Figure 4. Different responses to PEDV infection among the intestinal organoids

(A) Volcano plots showing differential gene expression (DEG) following PEDV infection, compared with mock-infected duodenal, jejunal, and ileal organoids. Gene that satisfied the threshold with an absolute log2 fold change ≥ 1 and *p*-values<0.05 were nominated as DEGs. (B) Bar graph showing the numbers of upregulated and downregulated DEGs in PEDV-infected organoids relative to the mock condition across the three intestinal regions. (C) Enriched Gene Ontology (GO) terms of the genes upregulated and downregulated following PEDV infection in duodenal, jejunal, and ileal organoids. (D–F) KEGG pathway enrichment analysis of genes significantly upregulated and downregulated in (D) duodenal, (E) jejunal, and (F) ileal organoids following PEDV infection. For KEGG pathway enrichment analysis, FDR<0.05 was used as cutoff threshold.

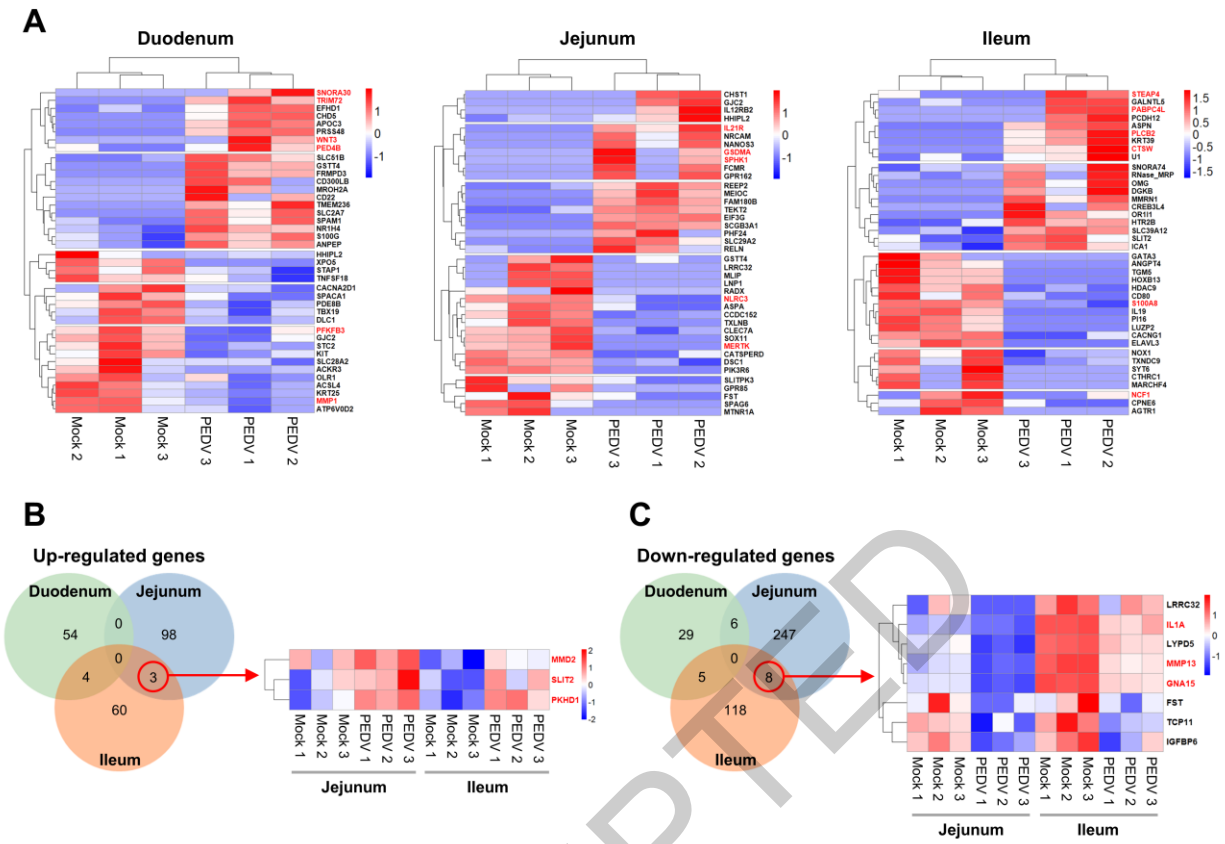

Figure 5. Factors influencing regional PEDV infection

(A) Heatmap of the top 20 genes upregulated and downregulated in PEDV-infected duodenal, jejunal, and ileal organoids, compared with the mock groups. Gene that satisfied the threshold with an absolute log2 fold change ≥ 1 and *p*-values<0.05 were nominated as DEGs. (B, C) Venn diagrams showing (B) upregulated genes and (C) downregulated genes in PEDV-infected duodenal, jejunal, and ileal organoids, compared with the mock groups. The heatmap below each Venn diagram displays the expression patterns of genes that were commonly upregulated and downregulated in both jejunal and ileal organoids, compared with the mock groups.